JACS
JOURNAL OF THE AMERICAN CHEMICAL SOCIETY

ARTICLE

pubs.acs.org/JACS

Neutral Histidine and Photoinduced Electron Transfer in DNA Photolyases

Tatiana Domratcheva*

Department of Biomolecular Mechanisms, Max-Planck Institute for Medical Research, Jahnstrasse 29, 69120 Heidelberg, Germany

Supporting Information

ABSTRACT: The two major UV-induced DNA lesions, the cyclobutane pyrimidine dimers (CPD) and (6−4) pyrimidine−pyrimidone photoproducts, can be repaired by the light-activated enzymes CPD and (6−4) photolyases, respectively. It is a long-standing question how the two classes of photolyases with alike molecular structure are capable of reversing the two chemically different DNA photoproducts. In both photolyases the repair reaction is initiated by photoinduced electron transfer from the hydroquinone-anion part of the flavin adenine dinucleotide ($FADH^-$) cofactor to the photoproduct. Here, the state-of-the-art XMCQDPT2-CASSCF approach was employed to compute the excitation spectra of the respective active site models. It is found that protonation of His365 in the presence of the hydroquinone-anion electron donor causes spontaneous, as opposed to photoinduced, coupled proton and electron transfer to the (6−4) photoproduct. The resulting neutralized biradical, containing the neutral semiquinone and the N3′-protonated (6−4) photoproduct neutral radical, corresponds to the lowest energy electronic ground-state minimum. The high electron affinity of the N3′-protonated (6−4) photoproduct underlines this finding. Thus, it is anticipated that the (6−4) photoproduct repair is assisted by His365 in its neutral form, which is in contrast to the repair mechanisms proposed in the literature. The repair via hydroxyl group transfer assisted by neutral His365 is considered. The repair involves the 5′base radical anion of the (6−4) photoproduct which in terms of electronic structure is similar to the CPD radical anion. A unified model of the CPD and (6−4) photoproduct repair is proposed.

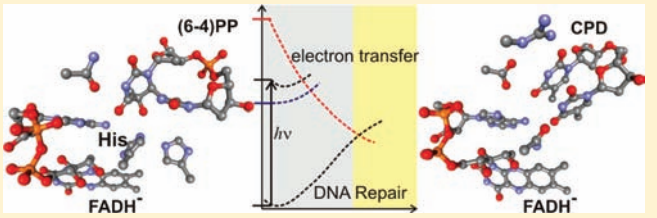

INTRODUCTION

Sun light can damage DNA structure by inducing covalent bonds between adjacent pyrimidine bases. The most common DNA photoproducts formed are cyclobutane pyrimidine dimers (CPD) and (6−4) pyrimidine−pyrimidone photoproducts (Chart 1). In many organisms, these lesions can be repaired by light-activated enzymes, the photolyases. Two types of photolyases specific for the repair of the (6−4) and CPD photoproducts have been identified and extensively studied (see refs 1−5 for recent reviews). Despite differing chemical structures of the photoproducts, the CPD and (6−4) photolyases share significant similarities in their overall molecular structure and repair mechanism. In both photolyases, after binding to the damaged DNA, the repair process consists of three consecutive steps. At first, the electronically excited hydroquinone-anion part of the flavin adenine dinucleotide ($FADH^-$) cofactor donates an electron to the photoproduct yielding the two radical species: the neutral flavin semiquinone radical and the anionic photoproduct radical. Then the photoproduct radical anion is reversed to a pair of undamaged DNA bases. Finally, radical recombination takes place via return electron transfer restoring the flavin hydroquinone anion.

The ring-opening in the CPD radical is fairly well understood,[6−8] whereas the chemical reaction underlying the (6−4) photoproduct repair remains unknown. For years, it was anticipated that the (6−4) photoproduct was repaired in the form of the oxetane intermediate (Chart 1) with a four-membered ring structure similar to CPD.[9,10] Recently, on the basis of structural[11−13] and spectroscopic data,[14] the original oxetane repair model was questioned and several new proposals were put forward,[11,12,14−16] stimulating extensive debate. Mechanistic hypothesis, originating from experimental[14] as well as theoretical[16] studies, considers the neutral radical of the N3′-protonated (6−4) photoproduct (Chart 1) as a critical repair intermediate instead of the oxetane. The atom numbering used in the text is indicated in Chart 1.

Recently reported crystal structures of the photolyases in complexes with different DNA photoproducts[11−13,17] show that the lesions are bound in close proximity to adenine and flavin of $FADH^-$. The conserved residues Glu283 and His365, interacting with the CPD and (6−4) photoproducts, respectively, were proposed to be protonated.[11,17] The significance of Glu283 and His365 for the photorepair reaction was demonstrated by mutagenesis studies.[11,18,19] The photodynamics of DNA repair by photolyases was studied in detail by means of ultrafast fluorescence upconversion and transient UV−vis absorption techniques.[14,20] The time constants of photoinduced electron transfer were determined to be 170 and 225 ps in the CPD[20] and (6−4) photolyases,[14] respectively. The subsequent photoproduct-repair steps required more than 500 ps in both photolyases.[14,20] Notably, in the (6−4)

Received: April 29, 2011
Published: October 03, 2011

ACS Publications © 2011 American Chemical Society

Chart 1. Photoproducts of Two Thymine Bases and Hypothetical Repair Intermediates

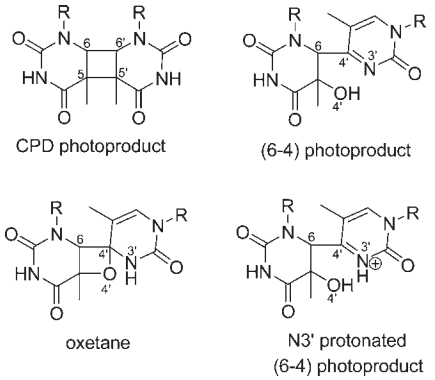

photolyase the repair step was found to be competing with the fast return-electron transfer, characterized by a rate constant of 50 ps.[14] Coexistence of the repair-efficient and futile electron-transfer cycles apparently results in the modest repair quantum yield.[14] Only a repair-efficient electron-transfer cycle was observed in the CPD photolyase. Accordingly, the enzyme works with a high repair quantum yield,[21] which is notably reduced in the Glu283/Ala mutant.[19]

Enzymatic repair of the (6−4) photoproduct is rather inefficient and takes place only in the presence of His365.[11,18] Mutations of this residue, as well as its neighbors, were detrimental for the repair function.[11,18] However, the futile electron-transfer cycle was still observed in the various His365 mutants.[14] At first, on the basis of the titration experiments,[18,22] it was proposed that His365 was protonated and that it might be involved in formation of the oxetane intermediate that takes place upon DNA binding to the enzyme. Recent X-ray crystal structures[11−13] and ultrafast spectroscopy studies[14] ruled out the oxetane formation preceding photoinduced electron transfer. Instead it was anticipated that the (6−4) photoproduct, rather than oxetane, accepts an electron from the electronically excited flavin.[11−14] Kinetic isotope effect was reported for the repair reaction in D_2O.[14,18] Given that His365 was found indispensable for repair, it was proposed that this residue might be involved in a catalytically critical proton transfer to the (6−4) photoproduct radical anion.[14]

Recent experimental data stimulated theoretical studies addressing the photorepair mechanism. Several quantum chemical studies have been published;[15,16,23] however, no common repair mechanism is emerging. In our previous work,[15] a repair pathway was identified that involves OH transfer in the electronically excited (6−4) photoproduct radical anion. Later, Harbach et al.[23] argued that photoexcitation of the $FADH^-$ would not deposit enough energy to populate the excited (6−4) photoproduct radical anion; therefore, the repair should occur in the radical-anion ground electronic state. Recently, Sadeghian et al.[16] reported a repair pathway corresponding to a two-photon process and involving an oxetane intermediate. None of these computational studies addresses all repair steps on equal footing, which is essential to draw final conclusion about the repair mechanism.

In terms of electronic structure, photoexcitation promotes electrons from bonding π to antibonding π^* molecular orbitals (MOs) of the flavin chromophore. Since this excitation involves only MOs localized on the chromophore, the respective excited state is termed a locally excited (LE) state. Another excited state corresponds to an electronic excitation resulting in intermolecular electron transfer from a π MO of the flavin electron donor to a virtual MO of the electron acceptor, e.g., the DNA photoproduct. This excited state is thus termed an electron-transfer (ET) state. Population of the ET state via the intersection with the LE state represents photoinduced electron transfer. The relative energies of the LE and ET states are of particular interest to study the photoinduced electron transfer in photolyases. In contrast to the bright LE states, the ET states have low oscillator strengths; therefore they are observed indirectly, e.g., by fluorescence quenching. The LE and ET excitation energies can be estimated by means of quantum chemical calculations. This computational task is rather challenging. A minimum quantum-mechanical system must include the electronic systems of both the chromophore/electron donor and the electron acceptor, and more than one excited state ought to be computed.

In this contribution, the effect of protonation on the electronic excitation spectrum of the photolyase active site is described for the first time. Rather large molecular models were computed using the state-of-the-art XMCQDPT2-CASSCF quantum-chemical approach.[24] It is demonstrated that protonated residues lower the excitation energies of the ET states, but not of the LE states of flavin. Remarkably, the lowest energy minimum of the protonated (6−4) photolyase active site has a biradical electronic structure; i.e., it contains the flavin semiquinone and the N3′-protonated (6−4) photoproduct radical in the electronic ground state. This result, corroborated by the high electron affinity of the N3′-protonated (6−4) photoproduct, predicts spontaneous, as opposed to photoinduced, proton coupled electron transfer upon photoproduct binding to the protonated active site.

The asymmetric structure of the (6−4) photoproduct results in two radical states localized on either the pyrimidone or pyrimidine bases. The higher energy radical state of the pyrimidine 5′base has an electronic structure similar to the CPD radical anion, and the corresponding ET states lie above the LE state of flavin. The OH-transfer repair[15] taking place in the presence of neutral His residues is considered. It is demonstrated that the energy of the pyrimidine 5′base radical decreases in the repair course. To search for the similarities between the two photolyases, the CPD and the (6−4) photoproduct electron affinities and the CPD and (6−4) photolyases' excitation spectra are compared. A unified mechanistic model of the CPD and (6−4) photolyases is formulated.

■ MOLECULAR MODELS AND COMPUTATIONAL DETAILS

The molecular models of the enzymatic active sites were constructed according to the X-ray crystal structures of photolyases pdb 1tez chain A [17] that contains the repaired CPD lesion and pdb 3cvu[11] that contains the (6−4) photoproduct. All residues forming hydrogen bonds with the photoproducts according to the crystal structures were included in the models; thus, the photoproducts were computed in their natural protein environment. The CPD and (6−4) photoproducts of the two N1-methyl thymine bases were considered. The amino acid side chains Glu283 and Asn349 interacting with the CPD were included in the CPD photolyase model; Glu283 was assumed to be protonated. The amino acid side chains His365, His369, and Gln299 interacting with the (6−4) photoproduct were included in the (6−4) photolyase models. Different protonation patterns were considered: four protonated models (6−4)I−IV and model (6−4), containing neutral His365 and His369. The flavin hydroquinone (HQ) moiety forms only one hydrogen bond with a conserved Asn residue in both photolyases, which was

Table 1. Computed Vertical Electron Affinities [kcal/mol (eV)] of the Thymine CPD and (6−4) Photoproducts[a]

photoproduct	electron affinity
(6−4) photoproduct, 3′base	6.0 (0.26)
N3′-protonated (6−4) photoproduct, 3′base	119.3 (5.17)
(6−4) photoproduct, 5′base	−16.7 (−0.72)
CPD	−11.6 (−0.48)

[a] The models are shown in Figure S1.

not included in the models. The HQ anion and N1-methyl adenine (Ad) were included and the sugar−phosphate part was omitted in the model of the $FADH^-$ cofactor. Cluster models were prepared by adding the hydrogen atoms to the crystal structure models using the HyperChem molecular modeling package.[25] Models (6−4)Int and (6−4)Repaired were obtained from model (6−4) by following the OH-transfer reaction coordinate. Quantum-chemical calculations were carried out with the Firefly program[26] which is partially based on the GAMESS US[27] source code.

The geometries of the active-site models were optimized by the B3LYP/6-31G(d) method, as detailed in the Supporting Information. The obtained geometries are in good agreement with the parent pdb models. In all models, the optimized geometry of the flavin ring system was found to be planar. At the optimized geometries, the excitation energies of the lowest lying singlet states were computed. The CIS calculations were used to identify the lowest lying excited states, and the energies were recomputed with the CASSCF and XMCQDPT2 methods (see the Supporting Information for details). The principal orbital CASSCF (POCAS) approach, described in our recent work,[28] was used in this study. The second-order MCSCF optimization method implemented in Firefly[26] was employed. State-averaged CASSCF calculations with equal weights for all roots were used. The effect of dynamic electron correlation on the excitation energies was accounted for by using the XMCQDPT2 method.[24] The standard 6-31G(d) basis set was used for the excitation energy calculations. To compare the closed-shell singlet and biradical energies, state-averaged CASSCF calculations were used with the active space consisting of the highest occupied molecular orbital (HOMO), localized on flavin, and the lowest unoccupied molecular orbital (LUMO), localized on either the 3′base or 5′base of the (6−4) photoproduct. Similarly, the unrestricted broken symmetry U-B3LYP calculations of models (6−4)II and (6−4)Int correspond to the HOMO−LUMO biradicals.

In addition to the supramolecular clusters, photoproduct models consisting of the two N1-methyl-thymine bases were computed at the B3LYP/TZVP level of theory. The models are shown in Figure S1 (Supporting Information). The geometries were optimized in the closed-shell singlet electronic state. At the singlet-state equilibrium geometries, the vertical electron affinities were determined as energy differences of the singlet and radical electronic states computed with the restricted (R-) and unrestricted (U-) B3LYP/TZVP methods, respectively.

RESULTS

1. Electron Affinities of the CPD and (6−4) Photoproducts. Table 1 contains the computed vertical electron affinities. The asymmetric structure of the (6−4) photoproduct results in two distinct radical states localized on either of the nucleotide bases.[15] The electron affinity of the aromatic pyrimidone 3′base is positive; that is, the corresponding radical anion is lower in energy than the neutral singlet molecule. The 3′base radical corresponds to the electronic ground state of the (6−4) photoproduct radical anion.[15] In contrast, the electron

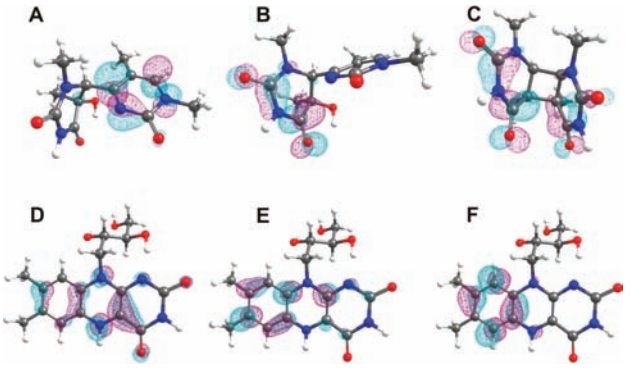

Figure 1. MOs involved in the photoinduced electron transfer in DNA photolyases: the singly occupied MOs of (A) the 3′base-(6−4) radical anion, (B) the 5′base-(6−4) radical anion, and (C) the CPD radical anion; the MOs of flavin hydroquinone anion, (D) the HOMO, (E) the LUMO, and (F) the LUMO + 1.

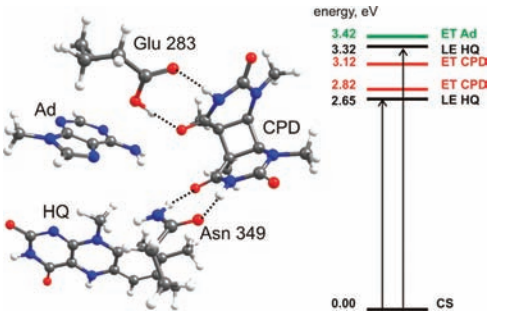

Figure 2. Optimized geometry and excitation spectrum of the CPD photolyase model. Dashed lines indicate hydrogen bonds. The vertical arrows show the local excitations in the UV−vis spectral range.

affinity of the pyrimidine 5′base is negative; that is, the corresponding radical anion is higher in energy than the neutral singlet molecule. To evaluate the electron affinity of the 5′pyrimidine base, which corresponds to the electronically excited state, a photoproduct model with the 3′base replaced by a methyl group was used. All photoproduct models are presented in Figure S1. Similar to the 5′base of the (6−4) photoproduct, the electron affinity of CPD is negative. The 5′base (6−4) and CPD radical anions have a similar electronic structure as shown in Figure 1B,C. Upon protonation of the N3′ atom, the electron affinity of the pyrimidone 3′base is increased by a factor of 20. As pointed out in the Introduction, several authors proposed the radical of the N3′-protonated (6−4) photoproduct to be the central intermediate in the repair reaction.[14,16] However, the high electron affinity of the N3′-protonated (6−4) photoproduct was not noticed until now.

2. Electronic Excitation Spectrum of the CPD Photolyase. The CPD photolyase model contains the neutral (protonated) Glu283 as suggested in previous studies.[8,17] The optimized geometry and the excitation spectrum are shown in Figure 2. Both Asn349 and protonated Glu283 form two hydrogen bonds with the CPD photoproduct. The hydrogen-bonding distances in the cluster and in the parent pdb structure are compared in Table S1 (Supporting Information). The electronic ground state has a closed-shell (CS) character (i.e., all electrons are paired) and contains a flavin HQ anion (two-electron reduced form) and

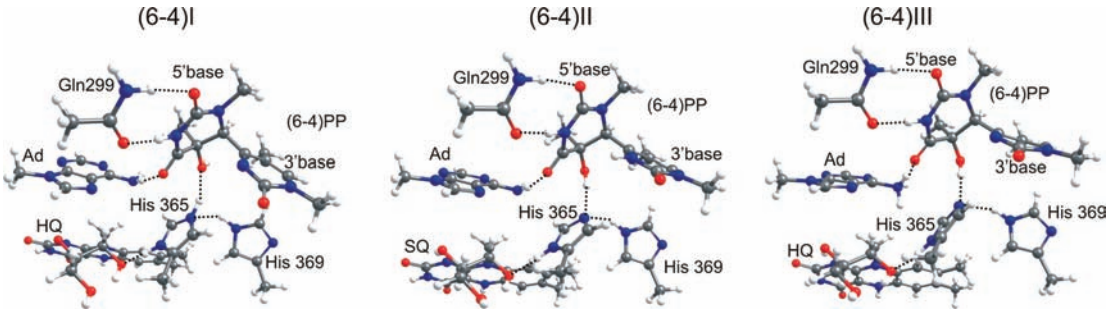

Figure 3. Optimized geometries of the protonated active sites: (6−4)I, protonated His365; (6−4)II, N3′-protonated 3′base; (6−4)III, protonated adenine. Dashed lines indicate hydrogen bonds.

Table 2. Relative Electronic Ground-State Energies [kcal/mol (eV)] of the (6−4) Photolyase Protonated Active Site Models[a]

model	R-/U-B3LYP	CASSCF(2,2)2	XMCQDPT2
(6−4)I	0.0	0.0	0.0
(6−4)II	−28.3 (−1.23)	−22.1 (−0.96)	−40.4 (−1.70)
(6−4)III	2.8 (0.12)		

[a] The absolute energies are listed in Table S10.

a neutral CPD photoproduct as expected for the photolyase active site before light absorption. The protocol developed to compute the excitation spectra is detailed in the Supporting Information. Full computational data on the CDP model are presented in Table S2 (Supporting Information). In the following the XMCQDP2 results are described and discussed for all computed models.

In the excitation spectrum (Figure 2), the two flavin LE states have energies 2.65 and 3.32 eV and the respective transition oscillator strengths are 0.07 and 0.28 (Table S2). Thus, the calculations predict that the flavin hydroquinone anion has a weak absorption around 470 nm and a stronger absorption around 375 nm. The prediction is in good agreement with the UV−vis spectrum of $FADH^-$ in photolyase[20] that has a maximum around 380 nm with a shoulder at the red side extending to about 500 nm. The absorption is attributed to the HOMO−LUMO and HOMO−(LUMO+1) transitions of the flavin HQ. The respective MOs are shown in Figure 1. The CASSCF-optimized active space MOs are shown in Figure S4 (Supporting Information). The three computed ET states involve either the photoproduct or the adenine ring. The two ET states of the photoproduct with energies 2.82 and 3.12 eV correspond to electron transfer predominantly to the 5′- and 3′base, respectively. The former is energetically favored because of the interaction with protonated Glu283. The ET state of the adenine ring is at 3.42 eV. Typically the oscillator strengths of the ET states are close to zero.

3. Electronic Excitation Spectrum of (6−4) Photolyase with Protonated His365. The three models (6−4)I−III shown in Figure 3 correspond to the protonated active site of the (6−4) photolyase. Model (6−4)I contains protonated His365 as originally proposed on the basis of titration experiments.[22] His365 via NδH is a proton donor in a hydrogen bond with O4′H of the (6−4) photoproduct. In Table S1 , the optimized distance between O4′H and protonated His365 is slightly elongated compared to the other models. The next model (6−4)II contains the (6−4) photoproduct protonated at the N3′position of the pyrimidone 3′base. Proton transfer from His365 to N3′ was proposed in recent mechanistic studies.[14,16] Model (6−4)III contains a protonated adenine fragment. Proton transfer from His365 to adenine is feasible because these two molecular fragments may interact in the absence of the photoproduct. The optimized geometries of the (6−4)II and III models are in good agreement with the parent pdb model (Table S1). For the sake of completeness, model (6−4)IV containing protonated His369 was also considered. The results are presented in Figure S5 and Table S7 in the Supporting Information. The ground-state energy and the excitation spectrum of model (6−4)IV are essentially similar to those of models (6−4)I and (6−4)III.

In Table 2, the energies of the isomeric (6−4)I−III models are compared in order to determine which protonation site is energetically favorable. The absolute energies are presented in Table S10 (Supporting Information). The (6−4)II model is a biradical (has two unpaired electrons in a singlet configuration) in the electronic ground state with an energy significantly lower than the energies of the closed-shell ground state of the (6−4)I and (6−4)III models. In the biradical, one unpaired electron is localized on the flavin semiquinone (one-electron reduced form), whereas the other unpaired electron is localized on the 3′base of the photoproduct. Thus, protonation of the photoproduct results in spontaneous electron transfer from $FADH^-$ and a significant stabilization of the active site in the biradical state. This new finding, with important implications for the repair mechanism, is not surprising if the high electron affinity of the protonated photoproduct (Table 1) is taken into consideration. In addition, all molecular fragments take their neutralized forms in the lowest energy minimum (6−4)II.

The excitation energies of models (6−4)I−III are presented in Figure 4. The computational data are presented in Tables S4−S6 in the Supporting Information. Relative positions of the electronic ground-state energies are chosen according to Table 2: the ground-state energy of models (6−4)I and -III are the same and set to zero, the ground-state energy of model (6−4)II is −40 kcal/mol (−1.7 eV) according to the XMCQDT2 results. The ground-state closed-shell models (6−4)I and -III are discussed and compared to the CPD model in the following. The first flavin LE state lies at 2.63 and 2.69 eV in models (6−4)I and -III, respectively, which is very close to the 2.65 eV in the CPD model. The second flavin LE state has an energy 3.27 or 3.32 eV in the (6−4)I or CPD models, respectively. Thus, the energy of the LE states of the flavin HQ is not affected by the environment, in particular by the protonated His365 and adenine. The ET state of the 3′base (6−4) photoproduct radical is below the first LE state of flavin, whereas the ET state of the 5′base, similarly to the ET state of CPD, is above the LE state. The (ET 3′base)−(ET 5′base)

energy gap, that is, the excitation energy of the (6−4) photoproduct radical anion, is 1.6 and 1.1 eV in models (6−4)I and -III, respectively; thus, it is sensitive to the photoproduct environment. The ET states of the protonated His and adenine are stabilized as compared to the neutral counterparts: The ET state of protonated His365 has an energy of 2.53 eV in model (6−4)I. The three ET states of the protonated adenine have energies 1.61, 2.82, and 3.01 eV in model (6−4)III.

According to the ground-state energies (Table 2), the protonated active site predominantly exists in the form of model (6−4)II; therefore, the excitation spectrum of the biradical rather than of the closed-shell models should be experimentally observed. The excitation spectrum of the (6−4)II biradical (Figure 4) contains the LE states of the flavin neutral semiquinone (SQ) and the neutral (6−4) photoproduct radical. The closed-shell state corresponds to the electronically excited state with the excitation energy comparable to the energy of the first LE state. Notably, the flavin semiquinone absorption in the photolyase was observed only transiently after photoexcitation,[14] and not in the electronic ground state as model (6−4)II predicts.

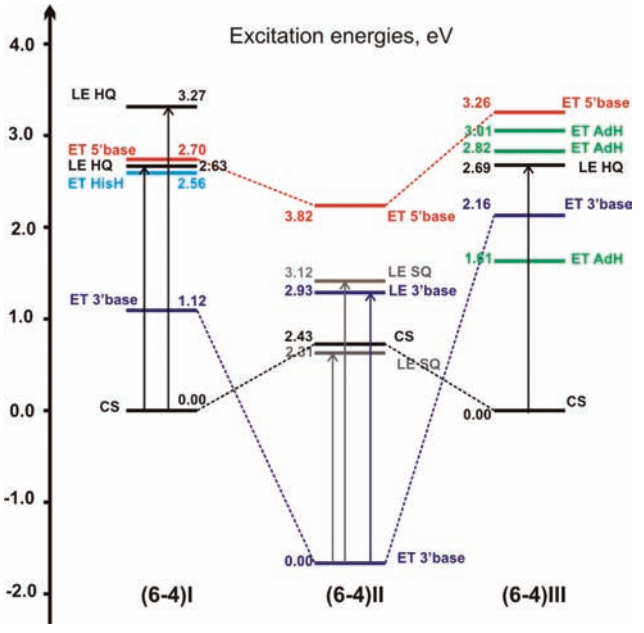

Figure 4. Energies of the protonated (6−4) models (Figure 3) in the electronic ground and excited states. The relative ground-state energies are set according to Table 2. The dashed lines connect the electronic states relevant to electron transfer between the flavin HQ anion and the (6−4) photoproduct. The excitation energies are indicated for each electronic state. The vertical arrows show the local excitations in the UV−vis spectral range.

The LE states of the flavin SQ radical are at 2.31 and 3.12 eV with the respective oscillator strengths 0.04 and 0.20. Thus, the calculations predict two absorption maxima in the visible range: a low intensity at 540 nm and a high intensity at 400 nm. The same MOs are involved in the HQ and SQ LE transitions as Figure S6 (Supporting Information) demonstrates. Experimentally, the absorption of the semiqinone radical in the photolyase was observed as broad peaks in the ranges of 300−400, 400−520, and 550−680 nm.[14] It is likely that the two computed LE states correspond to the 550−680 and 400−520 nm absorption peaks. The LE state of the 3′pyrimidone radical was found at 2.93 eV with the transition oscillator strength of 0.14. This LE state, corresponding to a $\pi\pi^*$ electronic transition of the 3′base radical, should be observed around 420 nm, which is significantly red-shifted compared to the absorption at 325 nm attributed to this photoproduct in the experimental study.[14] Therefore, it is unlikely that formation of the protonated (6−4) photoproduct radical was observed in the repair course. The energy of the 5′base radical anion lies at 3.82 eV. This excited state corresponds to an electron transfer between the two bases of the photoproduct radical and is characterized by a fairly weak transition oscillator.

4. Electronic Excitation spectrum of the (6−4) Photolyase with Neutral His365 and His369. The study of the models representing the protonated active sites reveals that protonated His365 is not compatible with photoinduced electron transfer. Therefore, it is anticipated that neutral His365 is present in the active site. The models shown in Figure 5 contain neutral His365 and His369 as NεH and NδH isomers, respectively. Model (6−4) represents the enzyme−substrate complex at the Franck−Condon geometry. His365 forms hydrogen bonds with His369 and the O4′H group of the (6−4) photoproduct. The optimized geometry of model (6−4) is in good agreement with the parent pdb model (Table S1).

In our previous work,[15] a repair pathway involving the transfer of the O4′H group from the 5′base to the 3′base was identified. Models (6−4)Int and (6−4)Repaired (Figure 5) represent an intermediate and the repaired structures, respectively, along the OH-transfer pathway. Model (6−4)Int was optimized with the CASSCF and U-B3LYP methods (see the Supporting Information for details). The ground electronic state of (6−4)Int is a biradical with unpaired electrons localized on the flavin ring and on the 5′base. The hydrogen bond between the "transferred" O4′H group and His365 is conserved. Structure (6−4)Int does not correspond to a local minimum at the U-B3LYP level of theory. Dissociation of the C6−C4′ bond concomitant with the electron transfer to the flavin ring, i.e., restoration of the

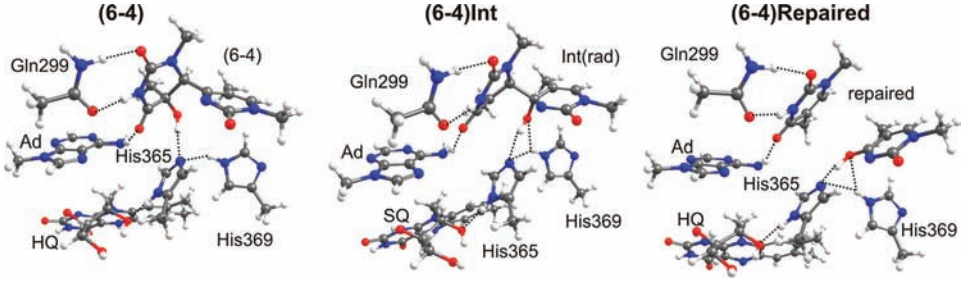

Figure 5. Optimized geometry of the (6−4) photolyase models containing two neutral His residues. Dashed lines indicate hydrogen bonds.

Table 3. Relative Electronic Ground-State Energies [kcal/mol (eV)] of the (6−4) Photolyase Active Site Models Containing Two Neutral His Residues[a]

model	R-/U-B3LYP	CASSCF(2,2)2	XMCQDPT2
(6−4)	0.0	0.0	0.0
(6−4)Int	54.6 (2.37)	65.2 (2.82)	42.4 (1.83)
(6−4)Repaired	−18.3 (−0.79)		

[a] The absolute energies are listed in Table S11 (Supporting Information).

closed-shell electronic configuration, was observed in the geometry optimization course leading to the local minimum (6−4)Repaired. Notably, model (6−4)Repaired contains the tautomeric 3′base which forms a hydrogen bond with His365 via the O4′H group. Thus, along the OH-transfer repair pathway the hydrogen bond His365−O4′H is conserved.

In Table 3, the relative energies of the structures along the OH-transfer repair pathway are collected; the absolute energies are given in Table S11 in the Supporting Information. The repair intermediate (6−4)Int is significantly higher in energy than the initial (6−4) structure, whereas the repair product (6−4)Repaired has a lower energy. For the three structures, the vertical excitation spectra were computed (full data are presented in Tables S3, S8, and S9 in the Supporting Information). The ground- and excited-state energies are compared in Figure 6. Relative energies of models (6−4)Int and (6−4)Repaired with respect to model (6−4) in the electronic ground state are set according to the XMCQDPT2 and U-B3LYP energies (Table 3), respectively. Note a drastic difference between the energy trends presented in Figure 6 and Figure 4. Whereas the energies in Figure 4 are consistent with the proton-coupled electron transfer in the electronic ground state, the energies in Figure 6 represent a typical photoreaction. In Figure 6, the ground state has a transition-state region, which is significantly elevated, whereas the energy of the red excited state, corresponding to the 5′base radical decreases, connecting the two ground-state minima (6−4) and (6−4)Repaired.

The computed excitation spectrum of model (6−4) comprises the two LE states of the flavin HQ with energies of 2.59 and 3.36 eV, the ET states of the 3′- and 5′base with energies of 2.06 and 3.77 eV, respectively, and the ET state of adenine with an energy of 3.61 eV. Full data are presented in Table S3. The energies of the LE states are in good agreement with the CPD model. The excitation energy of the photoproduct radical anion is 1.7 eV, which is in good agreement with the previously published calculations.[15,23] However, as demonstrated for the protonated models, the (ET 3′base)−(ET 5′base) energy gap varies significantly depending on the N3′-protonation state, on interactions within the active site, and also, as previously shown,[15] on the O4H−N3′ hydrogen bond between the two nucleotide bases.

In contrast to the other models computed in this work, model (6−4)Int represents an intermediate state transiently occurring in the repair course. In the electronic ground state, it contains two radicals—the neutral semiquinone and the 5′base-centered radical of the DNA repair intermediate. The corresponding CASSCF MOs are shown in Figure S8 in the Supporting Information. The (6−4)Int ground state correlates with the ET 5′base state of the (6−4) model as indicated in Figure 6. The energy of the 5′base radical at geometry

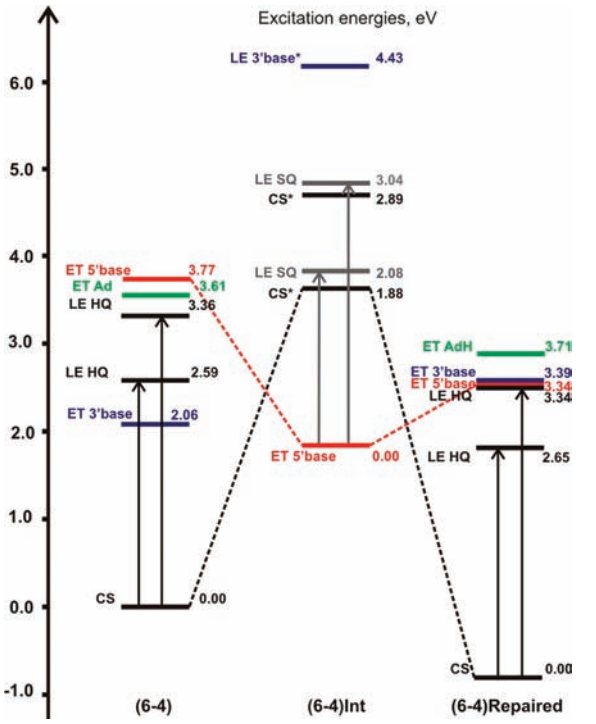

Figure 6. Energies of the models containing two neutral His residues (Figure 5) in the electronic ground and excited states. The relative ground-state energies are set according to Table 3. The dashed lines connect the electronic states relevant to the (6−4) photoproduct repair. The excitation energies are indicated for each electronic state. The vertical arrows show the local excitations in the UV−vis spectral range.

(6−4)Int is lowered compared to the energy of this state at the (6−4) geometry. In (6−4)Int, the radical 5′base is virtually neutral and the 3′base carries most of the negative charge (Table S12 in the Supporting Information). The locally excited state of the modified negatively charged 3′base (Figure 6) is found at 4.43 eV.

Although the ground state has a single-configuration character, the excitation spectrum of the (6−4)Int model is rather complicated due to the intermediate nature of this structure. The results of calculations are presented in Table S8 and Figure S8. The closed-shell configuration contributes to two excited states indicated as CS* in Figure 6 with energies of 1.88 and 2.89 eV. The two CS* states have a significant contribution of a configuration containing the closed-shell hydroquinone and a singlet open-shell photoproduct (each of the nucleotide bases has an unpaired electron). In addition, the CS* states interact with the locally excited semiquinone-radical states LE SQ with energies 2.08 and 3.04 eV (Figure 6). Generally, interacting electronic states represent a difficult case for electronic structure calculations. Nevertheless, the obtained LE-SQ energies in (6−4)Int are in agreement with those of the other biradical model (6−4)II which has a rather simple excitation spectrum.

The electronic excitations of the active site model (6−4)Repaired (Figure 6), containing the repaired photoproduct (Table S9 and Figure S8) has two LE states of hydroquinone with energies of 2.65 and 3.34 eV. Note the consistent results for the LE-HQ energies obtained with all models which have closed-shell ground-state structures. There are three ET states in the excitation spectrum. The ET states of the repaired 3′base and 5′base are found at 3.34 and

Scheme 1. Proposed OH-Transfer Repair Pathway[a]

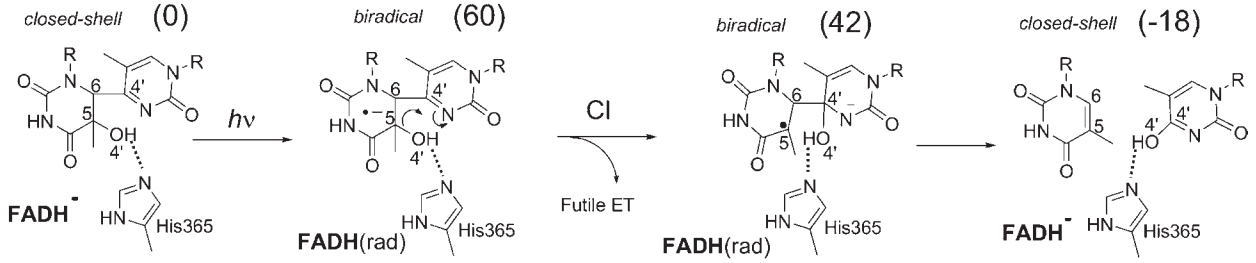

[a] The relative energies of the molecular complexes in kilocalories per mole are indicated in brackets according to Figure 6.

3.39 eV. The ET state of the adenine ring is at 3.71 eV, which is in good agreement with the excitation energy of this state at the initial geometry (6−4).

DISCUSSION

On the basis of the crystal structures of the CPD and (6−4) photolyases, different molecular models of the active sites were constructed. The models are rather large and are suitable to study photoinduced electron transfer because they include the flavin chromophore and the DNA photoproducts in their native environment. The geometries were optimized with attention paid to conserve the relative arrangement of the molecular fragments. The electronic excitation spectra were computed using a two-step approach. First, the CIS method was used to identify the low-lying electronic states. All excited electronic states relevant to this study have a single-electron excitation character and the CIS calculations provide a reasonable description of their relative energies as demonstrated in Figure S3. Then, the electronic states of interest were selected and their energies were recomputed using the XMCQDPT2-CASSCF approach. The obtained excitation spectra were used to compare the CPD- and (6−4)-repair active sites, to study the effect of protonated His365 on photoinduced electron transfer, and to follow the electronic structure and energy changes along the OH-transfer repair pathway.

1. Computed Electronic Excitation Spectra. The computed models provide a consistent picture of the flavin hydroquinone anion absorption properties. Two locally excited states were found in the energy ranges of 2.59−2.69 and 3.27−3.36 eV. The corresponding absorption maxima are in good agreement with the experimental spectrum.[14,20] The lowest energy transition in hydroquinone has a small oscillator strength. Therefore, the excited $FADH^-$ in photolyase is populated by using the energy transfer from an additional antenna chromophore. The computed energies of the LE states of the flavin semiquinone radical in models (6−4)II and (6−4)Int also nicely agree with the observed semiquinone absorption.[14,20] In addition, this study predicts, for the first time, that the N3′-protonated (6−4) photoproduct radical has an absorption peak in the visible range around 420 nm due to the $\pi\pi^*$ electronic transition in the neutral pyrimidone radical.

The XMCQDPT2-CASSCF method describes the LE and ET states on equal footing; therefore it is an adequate approach to study photoinduced electron-transfer reactions. In this study, advantage was taken of the very efficient XMCQDPT2-CASSCF code in Firefly.[26] In our recent paper,[28] the XMCQDPT2-CASSCF calculations were used to study the photoinduced electron transfer in a flavin-based blue-light photoreceptor. There we compared the computed energies of the ET states available in the literature.[28] In flavin-based photoreceptors, the ET states populated upon flavin photoexcitation typically lie above the first LE state of flavin.[28] The XMCQDPT2-CASSCF method predicts somewhat higher excitation energies of the ET states compared to the results of the CC2, MRCI(SD), and SOS-CIS(D) calculations.[28]

The computed models demonstrate how the ground- and excited-state energies depend on the protonation states of the active site. Whereas the excitation energies of the LE states of hydroquinone do not change, the ET states of the photoproduct are stabilized by interactions with the protonated hisitidines or adenine. In addition, the ET states of the protonated histidines or adenine appear among the low-lying electronic states. In the case of model (6−4)II, the ET state of the protonated 3′base is the electronic ground state. Comparison of models (6−4)I and -II reveals that the ET 3′base state is stabilized upon protonation by 65 kcal/mol which in fact equals the energy of the absorbed photon. The obtained results suggest that the protein environment and the charge distribution of the DNA fragment may influence the relative energies of the LE and ET states of the active site. These factors should be considered in a more realistic model by using combined quantum mechanical/molecular mechanical (QM/MM) calculations which are currently in progress. Nevertheless, the presented study already provides a valuable insight, because for the first time all electronic states relevant to the repair process are computed facilitating the discussion on the electronic structure of DNA repair.

2. 5′base Radical of the (6−4) Photoproduct Similar to the CPD Radical. There are two radical anions associated with the (6−4) photoproduct. The 3′pyrimidone radical anion has a positive electron affinity and corresponds to a stable molecular species.[15] The 5′pyrimidine radical anion has a negative electron affinity and corresponds to the electronic excited state. The electronic structure and electron affinity of the 5′base radical of the (6−4) photoproduct is similar to that of the CPD photoproduct. As demonstrated in our previous work,[15] the repair reactions of the (6−4) photoproduct radical anion via oxetane or via OH transfer involve the formation of the 5′base radical. The oxetane pathway, however, requires proton transfer to the N3′atom, further stabilizing the 3′base radical which is unfavorable for repair. The OH-transfer repair avoids N3′ protonation. Along this pathway, the energy of the 5′base radical decreases in a similar fashion as the energy of the CPD radical anion decreases upon the ring-opening repair reaction coordinate.[6−8] Therefore, despite the apparently differing chemical structures, striking similarities exist between the 5′base of the (6−4) and CPD

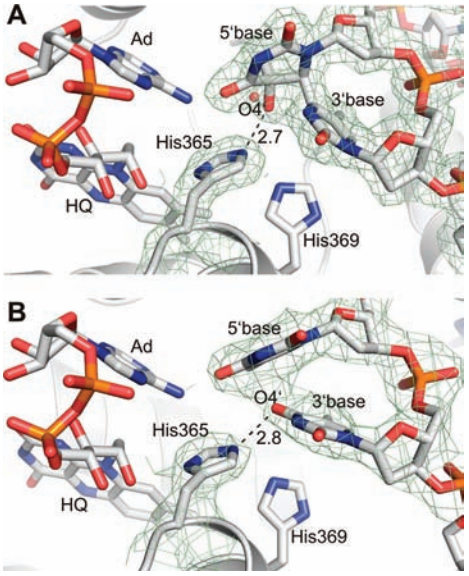

Figure 7. Crystal structures of the (6−4) photolyase (A) before repair pdb 3cvu [11] and (B) after repair pdb 3cvy.[11] The experimental 2mFo-DFc electron density map is shown (see the Supporting Information of ref 11 for details). The hydrogen-bond distances (Å) are indicated.

radical anions which underline the common repair by means of photoinduced electron transfer.

3. Repair of the (6−4) Photoproduct via OH Transfer. The repair reaction assisted by the neutral His365 is presented in Scheme 1. The chemical structures are consistent with the models in Figure 5, and the energies (indicated in brackets) are assigned according to the results of Figure 6. It is postulated that the repair starts from the 5′base radical of the photoproduct which has the energy of the absorbed photon 60 kcal/mol, i.e., the energy of the LE HQ state in model (6−4). The C5−O4′ bond in the 5′base dissociates, and the C4′-O4′ bond in the 3′base is formed. Along this reaction coordinate, the energy of the 5′base radical decreases and a crossing of the 5′base and 3′base radical states is reached.[15] Thus, a conical intersection (CI) rather than a transition state mediates the repair reaction. The conical intersection causes the pathway branching into futile and repair-efficient electron-transfer cycles as observed in the (6−4) photolyase. After OH transfer, the biradical (in the electronic ground state) undergoes return electron transfer as found in model (6−4)Int. The C6−C4′ bond dissociates yielding the repaired thymine bases and the reduced flavin.

According to the experimental data,[14] the repair channel is accessible only in the presence of His365. The crystal structures of the (6−4) photolyase containing DNA before and after repair[11] suggest that the hydrogen bond of His365 with the O4′H is conserved in the repair course, as illustrated in Figure 7. Structures (6−4) and (6−4)Repaired are in good agreement with the experimental structures (Table S1). It is reasonable to suggest that this hydrogen bond is critical for opening the OH-transfer repair channel. Indeed, the His365Asn mutant cannot repair DNA,[11,14] and no hydrogen bond between the Asn side chain and the O4′H group can be assumed according to the crystal structure of the mutant pdb 3cvw.[11] The futile electron-transfer cycle observed in the wild type as well as in the His365 mutants[14] may correspond to another relaxation path of the (6−4) photoproduct radical which is independent from the O4′H-His365 hydrogen bond and which involves the 3′base rather than 5′base radical state. Electronic structure studies on the 5′base radical relaxation, including the 5′base/3′base radical state crossing (identified in ref 15) are necessary to clarify this matter.

4. Protonated His365 and Proton-Coupled Electron Transfer. As the obtained results demonstrate, the N3′ protonation has a vast stabilization effect on the 3′base pyrimidone radical system. The lowest energy state of the protonated (6−4) photolyase, which corresponds to model (6−4)II, is found to comprise flavin semiquinone and the N3′-protonated 3′base-centered (6−4) photoproduct radical. Radical formation in this case takes place in the electronic ground state without photoexcitation. Therefore, a proton-coupled electron transfer (PCET) in the electronic ground state is predicted to take place upon the photoproduct binding to the protonated active site. All oxetane-involving repair models imply N3′ protonation, and therefore, should consider the formation of a stable (6−4)II-like biradical intermediate. The existence of this minimum causes the oxetane pathway to be incompatible with the photoinduced electron-transfer process and explains why the oxetane reaction coordinate is not exploited in the photolyase.[11,14] In line with this explanation, no hydrogen bonds involving the N3′ position of the 3′base is observed in the (6−4) photolyase crystal structures.[11−13]

5. Comparison of the Proposed (6−4) Photoproduct Repair Mechanisms. A repair mechanism involving the N3′-protonated (6−4) photoproduct was recently proposed by Sadeghian et al.[16] on the basis of combined QM/MM calculations. A two-step two-photon repair mechanism was derived. At first, protonation of the 3′base radical anion of the (6−4) photoproduct in the electronic excited state yields oxetane in the electronic ground state. The oxetane is repaired by another photoinduced electron transfer from flavin. There is a significant disagreement between the results of Sadeghian et al.[16] and the present study. In ref 16, it was found that N3′ protonation of the photoproduct radical decreases its energy by 22 kcal/mol. In this study the corresponding energy was found to be 65 kcal/mol (Figure 4, "blue" state in models (6−4)I and (6−4)II). The significant stabilization of the photoproduct radical upon N3′ protonation is explained by the significantly increased electron affinity (Table 1) causing PCET. The intrinsic property of the protonated pyrimidone base, such as electron affinity, should be similarly reproduced in the QM/MM calculations of ref 16 and in the cluster models presented here. Therefore, according to the results of this study, the calculated relative energies of the repair intermediates in ref 16 may contain an error. Consequently, the energy barrier for the return electron transfer and oxetane formation in ref 16 may be vastly underestimated.

A repair mechanism involving "transient" oxetane was proposed by Li et al.[14] to explain the observed ultrafast photodynamics of the repair process. Protonated His364 (analogous to His365 of this study) is suggested to assist the oxetane formation in the radical state after the photoexcitation.[14] This proposal is at odds with the results of this study which predicts PCET in the electronic ground state, i.e., without photoexcitation, due to protonated His365. In addition, presently it is entirely unknown whether the postulated "transient" oxetane[14] exists and whether its energy is comparable to the energy of the photon. The oxetane radical proposed by Li et al.[14] has a zwitterionic electronic structure. It contains a 5′base-centered radical anion and the N3′-protonated 3′base cation. In our previous work,[15] we demonstrated that in the radical state the oxetane corresponds to a transition state rather than to a

minimum. According to this work, it should be considered that elongation of the O4′−C4′ bond in the zwitterionic oxetane depicted in ref 14 leads to a (6−4)II-like structure, i.e., the neutral N3-protonated 3′base radical in which both the electron and the proton belong to the same pyrimidone ring. The formation of the neutralized biradical has a huge energetic advantage according to the data of Figure 4 and must constitute the main relaxation pathway aborting the repair reaction. The latter consideration contradicts the experimental mechanistic model of ref 14, which assumes that the zwitterionic oxetane has only one relaxation pathway toward the repair product. Thus, the "transient oxetane" repair model is inconsistent with electronic structure calculations, despite its apparent capability to account for the observed H/D effect and the critical role of His364.[14] The latter was proposed to be a proton donor to the photoproduct in the repair process.[14] An accelerated decay of the transient absorption signal and the lower steady-stay repair quantum yield in D_2O were explained by the slower deuteron-transfer repair step.[14]

The OH-transfer repair model avoids protonation of the photoproduct, apparently contradicting the experimental data of Li et al.[14] However, it implies an alternative explanation for the reduced repair quantum yield. In the deuterated active site, the pathway branching into futile and repair efficient pathways on the conical intersection might be altered without slowing-down the repair step. Because of the complexity and the size of the problem, here we step on entirely unexplored ground, and further computational and experimental studies are necessary to develop and confirm the OH-transfer repair hypothesis or to rule it out. In addition, the properties of the photoproduct radical anion as well as its N3′-protonated counterpart deserve a careful study, not only by calculations but also by experiment.

6. Unified Model of the CPD and (6−4) Photoproduct Repair. Figure 8 summarizes the mechanism of the repair process emerging from the present study and our previous work.[15] The active site model (6−4) containing neutral His365 is considered. The computed excitation spectrum is shown. The second LE HQ and ET Ad states (Figure 6) are omitted for clarity. The dashed lines indicate the expected relaxation energy curves. The Franck−Condon (ET 5′base)−(LE HQ) energy gap is about 1 eV. The fact that the ET state has a higher energy than the LE state at the Franck−Condon geometry does not mean that there is an energy shortage for the photoinduced electron transfer to the 5′base, as it was falsely declared by Harbach et al.[23] The conclusion of ref 23 would be correct if it had been grounded on adiabatic rather than vertical energies. In particular the relaxation of the 5′base radical anion along the repair coordinate should be taken into account in ref 23.

The critical points defining the photorepair dynamics are indicated as 1−4 in Figure 8. Point 1 corresponds to the energy obtained by photon absorption. The energy of the LE/ET crossing 2 corresponds to the upper bound of the activation energy of the photoinduced electron transfer. In Scheme 1 this energy is postulated to be equal to the energy of the LE HQ state at the Franck−Condon geometry. The decrease of the ET energy after 2 along the repair coordinate, e.g., the O4′H-group transfer, determines the driving force of the process. Because the 3′base radical state is below the LE state, the relaxation proceeds via the 3′base/5′base radical state crossing 3. After geometry 3, either the 3′base radical or the 5′base radical is formed. The branching ratio at 3 determines the futile/repair electron-transfer branching observed in the (6−4) photolyase.

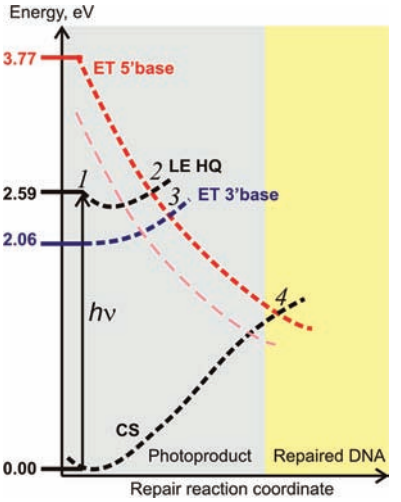

Figure 8. Photorepair energy diagram showing the vertical excitation spectrum of the active site and the expected energy changes along the repair pathway. Photon absorption corresponds to (1). (2) Photoinduced electron transfer and formation of the 5′base photoproduct radical anion, (3) crossing of the radical anion electronic states ET 5′base and ET 3′base mediates the repair reaction, and (4) crossing of the ET 5′base state and the closed shell (CS) ground state. The thin pink curve indicates the stabilized ET state crossing the CS ground state before the repair reaction is completed. The gray and yellow backgrounds correspond to the photoproduct and the repaired DNA valleys, respectively, on the electronic ground-state potential energy surface.

The 5′base radical undergoes repair reaching geometry 4, where the ground and excited states cross, leading to either formation of a biradical intermediate in the electronic ground state or radical recombination and return electron transfer to flavin. The former is represented by model (6−4)Int. After geometry 4, relaxation of the biradical yields the repaired DNA and reduced flavin.

A similar energy diagram as in Figure 8 explains the CPD repair as well. The ET CPD state corresponds to the ET 5′base state. There is no underlying state like the ET 3′base state; therefore, there is no state crossing 3 to consider. Thus, the CPD repair is determined by points 1, 2, and 4. The repair coordinate is the opening of the CPD ring via consecutive dissociation of the C5−C5′ and C6−C6′ bonds.[6−8] Here note the similarity between the C5−O4′ bond dissociation in the OH-transfer repair and the C5−C5′ bond dissociation in the CPD ring opening, which is explained by the similar electronic structure of the respective radical anions (Figure 1B,C).

The location of geometry 4 along the reaction coordinate determines the repair quantum yield. Specifically, for successful repair the crossing should occur after the transition state in the electronic ground state (indicated as the gray−yellow border in Figure 8). It is noteworthy that, in the CPD photolyase active site (Figure 2), the ET state is only 0.2 eV above the LE state, which is much lower compared to the ET 5′base state of the (6−4) photolyase. The stabilized ET state, e.g., lowered in energy by interactions with a protonated side chain, is indicated as the pink curve in Figure 8. The diagram suggests that the stabilized ET state (the pink curve) may cross the closed-shell state on the gray background, i.e., before the repair is completed. In such a case, the relaxation in the ground state leads to the structure containing the DNA photoproduct rather than the repaired

DNA. In the case of the pink ET curve, photostability instead of photorepair is expected. Thus, the relative energy of the ET state is directly connected to the repair quantum yield. It is important to note that crossing 4, determining the repair quantum yield in the CPD photolyase, has not been studied yet, which is especially interesting for understanding the reduced quantum yield of the mutated enzyme.[19]

CONCLUDING REMARKS AND OUTLOOK

The repair of the CPD and (6−4) photoproducts by the respective photolyases can be interpreted as a flavin-based photocycle. Photoactivation of flavin leads to electron transfer and transient formation of radical species whose structural relaxation results in DNA repair, and finally, radical recombination via a return electron transfer to flavin. A generalized energy diagram for this process is depicted in Figure 8. Apparently, molecular mechanisms which are consistent with this type of photocycle are widely employed in biology, e.g., in polypeptide and DNA-base photostability[29,30] and in flavin-based photoreceptors.[28] Computations of the entire pathway 1−4 in photolyases will result in grasping the determining factors of such processes. In this study, the excitation spectra were analyzed, which is the first step in calculating the entire electron-transfer cycle. The XMCQDPT2-CASSCF computational approach to the problem is established. Importantly, this approach provides an access to the relaxation pathways in electronic excited states and state crossings.

Here, the models of the (6−4) photolyase protonated active site, the models along the OH-transfer repair pathway, and the comparison of the (6−4) and CPD photolyases are presented. Unexpectedly it is found that the protonated active site of the (6−4) photolyase is not compatible with photoinduced electron transfer: In the presence of protonated His365, spontaneous electron transfer coupled to proton transfer takes place which is driven by the high electron affinity of the N3′-protonated (6−4) photoproduct. This finding calls for reexamination of the current mechanistic models involving protonated His365 and N3′-protonation of the (6−4) photoproduct.[11,14,16] In contrast, the OH-transfer repair model[15] looks very promising because it avoids N3′-protonation, thereby opening a new direction in DNA mechanistic studies. In addition, an interesting insight was gained from the comparison of the CPD and (6−4) models. Similarities were found between the 5′base radical of the (6−4) photoproduct and the CPD radical anion and between the OH-transfer repair and the CPD ring opening explaining the common repair mechanism.

ASSOCIATED CONTENT

Supporting Information. Text describing computational protocols for the restrained geometry optimization and the excitation energy calculations, figures showing models of the photoproducts used, enzymatic active sites according to crystal structures, electronic excitation spectra, CASSCF-optimized MOs, and optimized geometry and vertical spectrum of model (6-4)IV, tables listing optimized geometries compared with parent pdb models, models CPD, (6-4), (6-4)I, (6-4)II, (6-4)III, (6-4)IV, (6-4)Int., and (6-4)Repaired, total electronic energies, charge and spin distributions, and Cartesian coordinates of the optimized geometries, and a chart showing atom numbering in the OH-transfer repair intermediate. This material is available free of charge via the Internet at http://pubs.acs.org.

AUTHOR INFORMATION

Corresponding Author
Tatjana.Domratcheva@mpimf-heidelberg.mpg.de

ACKNOWLEDGMENT

I am very grateful to Chris Roome for the excellent high-performance-computing support, to Ilme Schlichting for long-term collaboration, support, and critical reading of the manuscript, to Anikó Udvarhelyi for useful suggestions, to Thomas Barends for preparing Figure 7, to Massimo Olivucci (University of Siena, Bowling Green State University) for inspiring discussions, and to Thomas Carell (LMU Munich) for opportunities to present and discuss my work in the excellent scientific setting of the DFG-SFB479 symposium. The financial support from the MPG Minerva program is gratefully acknowledged.

REFERENCES

(1) Sancar, A. *Chem. Rev.* **2003**, *103*, 2203–2237.
(2) Sancar, A. *J. Biol. Chem.* **2008**, *283*, 32153–32157.
(3) Muller, M.; Carell, T. *Curr. Opin. Struct. Biol.* **2009**, *19*, 277–285.
(4) Essen, L. O.; Klar, T. *Cell. Mol. Life Sci.* **2006**, *63*, 1266–1277.
(5) Weber, S. *Biochim. Biophys. Acta* **2005**, *1707*, 1–23.
(6) Harrison, C. B.; O'Neil, L. L.; Wiest, O. *J. Phys. Chem. A* **2005**, *109*, 7001–7012.
(7) Masson, F.; Laino, T.; Tavernelli, I.; Rothlisberger, U.; Hutter, J. *J. Am. Chem. Soc.* **2008**, *130*, 3443–3450.
(8) Masson, F.; Laino, T.; Rothlisberger, U.; Hutter, J. *ChemPhysChem* **2009**, *10*, 400–410.
(9) Kim, S. T.; Malhotra, K.; Smith, C. A.; Taylor, J. S.; Sancar, A. *J. Biol. Chem.* **1994**, *269*, 8535–8540.
(10) Zhao, X.; Liu, J.; Hsu, D. S.; Zhao, S.; Taylor, J. S.; Sancar, A. *J. Biol. Chem.* **1997**, *272*, 32580–32590.
(11) Maul, M. J.; Barends, T. R.; Glas, A. F.; Cryle, M. J.; Domratcheva, T.; Schneider, S.; Schlichting, I.; Carell, T. *Angew. Chem., Int. Ed.* **2008**, *47*, 10076–10080.
(12) Glas, A. F.; Schneider, S.; Maul, M. J.; Hennecke, U.; Carell, T. *Chem.—Eur. J.* **2009**, *15*, 10387–10396.
(13) Glas, A. F.; Kaya, E.; Schneider, S.; Heil, K.; Fazio, D.; Maul, M. J.; Carell, T. *J. Am. Chem. Soc.* **2010**, *132*, 3254–3255.
(14) Li, J.; Liu, Z.; Tan, C.; Guo, X.; Wang, L.; Sancar, A.; Zhong, D. *Nature* **2010**, *466*, 887–890.
(15) Domratcheva, T.; Schlichting, I. *J. Am. Chem. Soc.* **2009**, *131*, 17793–17799.
(16) Sadeghian, K.; Bocola, M.; Merz, T.; Schutz, M. *J. Am. Chem. Soc.* **2010**, *132*, 16285–16295.
(17) Mees, A.; Klar, T.; Gnau, P.; Hennecke, U.; Eker, A. P.; Carell, T.; Essen, L. O. *Science* **2004**, *306*, 1789–1793.
(18) Hitomi, K.; Nakamura, H.; Kim, S. T.; Mizukoshi, T.; Ishikawa, T.; Iwai, S.; Todo, T. *J. Biol. Chem.* **2001**, *276*, 10103–10109.
(19) Vande Berg, B. J.; Sancar, G. B. *J. Biol. Chem.* **1998**, *273*, 20276–20284.
(20) Kao, Y. T.; Saxena, C.; Wang, L.; Sancar, A.; Zhong, D. *Proc. Natl. Acad. Sci. U. S. A.* **2005**, *102*, 16128–16132.
(21) Kim, S. T.; Sancar, A. *Photochem. Photobiol.* **1993**, *57*, 895–904.
(22) Schleicher, E.; Hitomi, K.; Kay, C. W.; Getzoff, E. D.; Todo, T.; Weber, S. *J. Biol. Chem.* **2007**, *282*, 4738–4747.
(23) Harbach, P. H. P.; Borowka, J.; Bohnwagner, M. V.; Dreuw, A. *J Phys. Chem. Lett.* **2010**, *1*, 2556–2560.
(24) Granovsky, A. A. *J. Chem. Phys.* **2011**, *134*, 214113–214126.
(25) *Molecular modeling system.*, HyperChem Release 7.5 for Windows; Hypercube: Gainesville, FL, USA, 2002.

(26) Granovsky, A. A. Firefly version 7.1.G, www http://classic.chem.msu.su/gran/firefly/index.html. Access date: April 2011.
(27) Schmidt, M.; Baldridge, K. K.; Boatz, J. A.; Elbert, S. T.; Gordon, M. S.; Jensen, J. H.; Koseki, S.; Matsunaga, N.; Nguyen, K. A.; Su, S.; Windus, T. L.; Dupuis., M.; Montgomery, J. A. *J. Comput. Chem.* **1993**, *14*, 1347–1363.
(28) Udvarhelyi, A.; Domratcheva, T. *Photochem. Photobiol.* **2011**, *87*, 554–563.
(29) Shemesh, D.; Sobolewski, A. L.; Domcke, W. *J. Am. Chem. Soc.* **2009**, *131*, 1374–1375.
(30) Sobolewski, A. L.; Domcke, W.; Hattig, C. *Proc. Natl. Acad. Sci. U. S. A.* **2005**, *102*, 17903–17906.